Technical Innovations & Patient Support in Radiation Oncology 23 (2022) 27–32

Contents lists available at ScienceDirect

Technical Innovations & Patient Support in Radiation Oncology

journal homepage: www.sciencedirect.com/journal/technical-innovations-and-patient-support-in-radiation-oncology

Impact of transperineal ultrasound on perineal skin dose in prostate radiation therapy

Kalani De Silva [a], Amy Brown [b,*], Christopher Edwards [a]

[a] School of Clinical Sciences, Queensland University of Technology, Gardens Point Campus, Brisbane, QLD, Australia
[b] Townsville University Hospital, Townsville, Queensland, Australia

ARTICLE INFO

Keywords:
Prostate cancer
Image-guidance radiation therapy
Transperineal ultrasound
Prostate intrafraction motion

ABSTRACT

Introduction: This study investigated the relationship between anatomical compression introduced via ultrasound probe pressure and maximum perineum dose in prostate radiotherapy patients using the Clarity transperineal ultrasound (TPUS) system.
Methods: 115 patient ultrasound and computed tomography scans were retrospectively analysed. The probe to prostate apex distance (PPA), probe to inferior corpus spongiosum distance (PICS) and maximum perineum dose were calculated. Compression was represented by the PICS and the calculated corpus to prostate ratio (CPR). Demographics included treatment technique, image quality, body mass index (BMI) and age. Multiple linear regression analysis assessed the relationship between compression measures and perineum dose.
Results: The maximum dose to perineum ranged from 1.81 to 45.56 Gy, with a median of 5.87 Gy (Interquartile range (IQR) 3.17). The PICS distance and CPR recorded was 1.67 cm (IQR 0.63) and 0.51 (range 0.29–0.85) respectively. Regression analysis demonstrated both PICS and CPR were significant predictors of maximum dose to the perineum ($p < 0.001$). Patient-specific factors, including age, BMI, treatment technique and ultrasound image quality, were not factors that significantly impacted the maximum perineum dose.
Conclusion: There was a statistically significant association between increased anatomical compression and perineal dose measurements. A PICS of 1.2 cm or greater is recommended, with compression reduced as much as possible without losing anatomical US definition. Future investigations would be beneficial to evaluate the optimal balance between ultrasound image quality and transducer compression considering the perineum dose.

Introduction

A challenge in prostate radiation therapy treatment is positional changes during (intrafraction) and between (interfraction) treatments. Accurate prostate localisation is influenced by random inherent motion and the size and positional changes of the rectum and bladder [1]. This stochastic process increases position variance over time [2,3]. Intrafraction and interfraction motion increases the risk of geometric misalignment, causing compromised target coverage. and an undocumented dose distribution that can induce adverse effects in normal tissue [4,5].

The Clarity Autoscan System (Elekta Ltd, Missouri, USA) is a transperineal ultrasound (TPUS) system that monitors intrafraction prostate motion during dose delivery. The probe is housed on a motorised control arm and is stabilised on the patient's perineum throughout the radiation treatment [2]. (Fig. 1) Probe position reproducibility is achieved in the Clarity TPUS system through a visual guide providing real-time feedback of both probe angle and pressure, replicating the planned probe position (Supplementary Fig. 1). The Clarity system will pause dose delivery if the prostate deviates significantly from the required position during treatment. Intrafraction monitoring prevents surrounding organs at risk (OAR) from receiving higher doses and maintains the treatment intent according to the medical prescription [6]. The TPUS and associated set up is reported to be well-tolerated by patients [7,8].

Clarity TPUS is a non-ionising modality used for image-guidance. However, this benefit should not be counteracted in practice by increasing perineal dose with anatomical compression [3]. In typical male pelvis anatomy without ultrasound compression, the perineum

Abbreviations: TPUS, Transperineal Ultrasound; PPA, Probe surface to prostate apex distance; PICS, Probe surface to inferior corpus spongiosum distance; CPR, Corpus to the prostate ratio.

* Corresponding author at: Townsville University Hospital, PO Box 670, Townsville, QLD 4810, Australia.
E-mail address: Amy.Brown@health.qld.gov.au (A. Brown).

https://doi.org/10.1016/j.tipsro.2022.08.003
Received 10 June 2022; Received in revised form 9 August 2022; Accepted 15 August 2022
Available online 27 August 2022

area is usually not within a mid-high dose region with reported distances of 4.86 cm (1.38 cm SD; range 2.5–8) between the anal verge and prostate apex in 100 patients, and a median value of 5 cm (range: 3–7.5) in 95 patients [9]. However, clinical observations and research have demonstrated that structures, such as the perineum and penile bulb, can be shifted into higher dose regions due to anatomical compression via pressure applied by the TPUS probe [10–12]. Excessive dose can result in a painful, erythematous rash with moist desquamation that impedes patient quality of care [13].

We hypothesised that excessive anatomical compression due to TPUS probe position can result in increased and unintended doses to the perineum. This study investigated the dosimetric impact on perineal skin due to anatomical compression in prostate cancer patients using Clarity.

Method

Institutional ethics approval, including waiver of consent, was granted (HREC/2019/QTHS/58957). As per department protocol, patients undergoing a standard course of prostate radiation therapy with the Clarity Autoscan system would receive a planning scan followed by treatment with 78 Gray (Gy) in 39 fractions. The simulation session included TPUS and a computed tomography (CT) scan to visualise the prostate and surrounding anatomy. The TPUS was acquired with a 5.0 MHz transducer attached to the Clarity system. The planning CT used a Toshiba Aquilion LB CT scanner (Toshiba Medical Systems Corporation, Otawara, Japan) with 2 mm slices. The CT and TPUS scan data were individually imported into the treatment planning system (TPS), Monaco Version 5.11 (Elekta Ltd, Missouri, USA) and co-registered in absolute room coordinates.

Data collection

The study included 115 males who underwent prostate (+/- seminal vesicles) radiation therapy treatment with the Clarity Autoscan TPUS System. Patients were consecutively included, however excluded if hip prothesis artifact prevented accurate measurements on planning CT. Measurements were collected retrospectively from co-registered CT-ultrasound scans and the treatment plan. All patients were planned on Monaco V5.10 or V5.11 (Elekta Ltd, Missouri, USA), utilising a collapsed-cone algorithm and 10MV for three-dimensional conformal radiation therapy (3DCRT), and monte carlo algorithm and 6MV for both the intensity-modulated radiation therapy (IMRT) and volumetric modulated radiation therapy (VMAT) treatments. The treatment delivery was on Elekta Versa linear accelerators (Elekta Ltd, Missouri, USA). Standard image-guidance protocols for all patients included an initial daily-acquired TPUS match against the planning TPUS, and a cone-beam computed tomography scan (CBCT) to verify positioning and any OAR changes. CBCT matching was to prostatic fiducial markers or soft tissue where fiducial markers could not be inserted (due to factors such as reliance on anti-coagulants, patient refusal etc). Patient age at treatment, height and weight were collected retrospectively through the information management system, MOSAIQ (Elekta Ltd, Missouri, USA). Body mass index (BMI) was calculated (weight (kg)/height (m)^2).

Probe pressure could not be measured directly with a haptic sensor; therefore, surrogate tissue measurements were developed to investigate anatomical compression caused by the ultrasound probe. Departmental clinical observations during TPUS imaging demonstrated changes in the position of the inferior corpus spongiosum relative to the prostate apex when the RT operator positioned the probe. During probe placement, a reduction in corpus spongiosum thickness, a shifting of the inferior corpus spongiosum towards the prostate apex and a slight reduction in the distance of the probe surface to inferior corpus spongiosum occurred with increasing pressure. These clinical observations are supported by Pang et al. (2020), reporting a reduction in the effective scan path from the inferior prostate boundary to the skin when TPUS probe pressure was increased in the Clarity system [11].

The following measurements were collected from the patient's initial CT and ultrasound scan (Fig. 2): Probe surface to prostate apex distance (PPA) and probe surface to inferior corpus spongiosum distance (PICS). Additionally, to account for the change of inferior corpus spongiosum position relative to the prostate and its compression, a corpus to the prostate ratio (CPR) was calculated (Eq. (1)).

$$Corpus\ to\ prostate\ ratio\ (CPR) = \frac{Probe\ to\ inferior\ corpus\ spongiosum\ (PICS)\ distance}{Probe\ to\ prostate\ apex\ (PPA)\ distance} \quad (1)$$

Due to the shifting of the corpus spongiosum towards the prostate and its location inferior to the prostate apex, increasing probe compression reduced the PICS distance and resulted in a CPR approaching 1 (Fig. 2).

Maximum perineum dose

As per clinical guidelines, a perineum structure was created on CT for each dataset, defined as the portion of skin that extends 5 mm above the probe surface. To create the structure, the probe was contoured on CT. The TPS 'expansion and contraction' tool was used to expand the probe

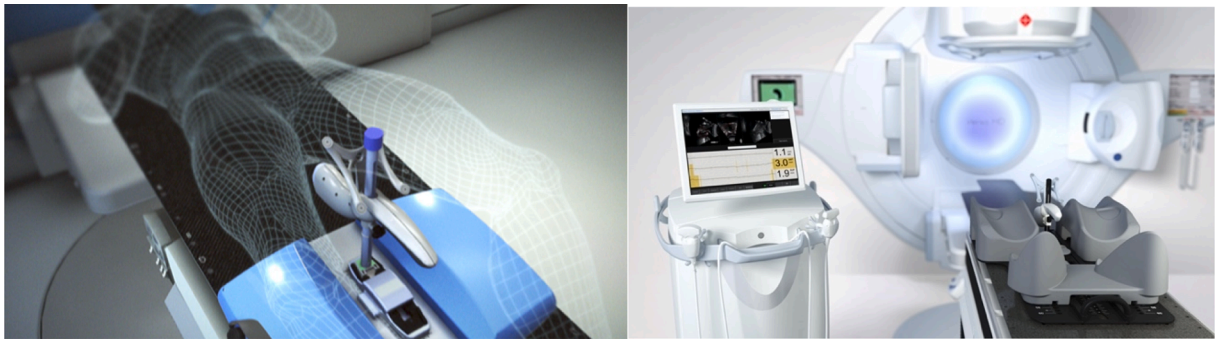

Fig. 1. Clarity Autoscan ultrasound set up during treatment (Reproduced with permission from Elekta Ltd).

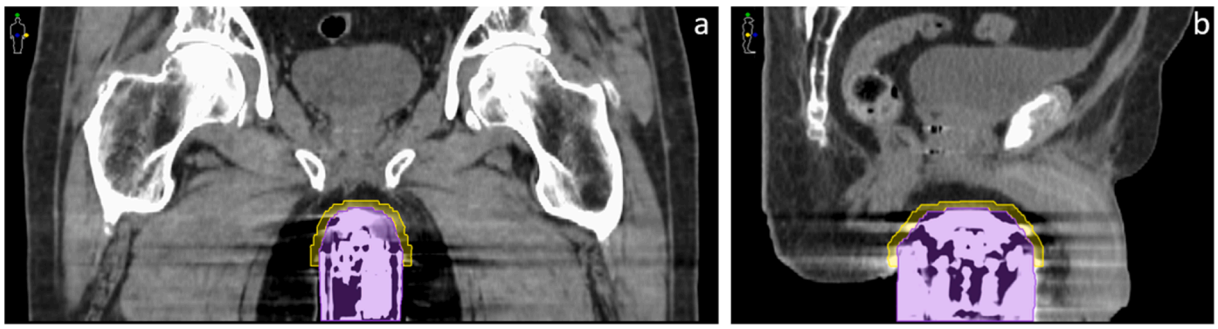

Fig. 2. Demonstration of the perineal structure (yellow) created on the planning CT in the treatment planning system from the probe (purple) in the coronal (a) and sagittal (b) planes. (For interpretation of the references to colour in this figure legend, the reader is referred to the web version of this article.)

structure by 5 mm to create a preliminary structure. The initial probe structure was then subtracted from the preliminary structure to achieve an outline of perineum skin (Fig. 2). The maximum perineum point dose in Gy was recorded.

Measurements

The probe surface was defined on the CT dataset at the most superior, transverse slice where the probe is visible. This location was confirmed in the sagittal and coronal CT planes using a fused ultrasound dataset. The reference point of the inferior corpus spongiosum was defined as the

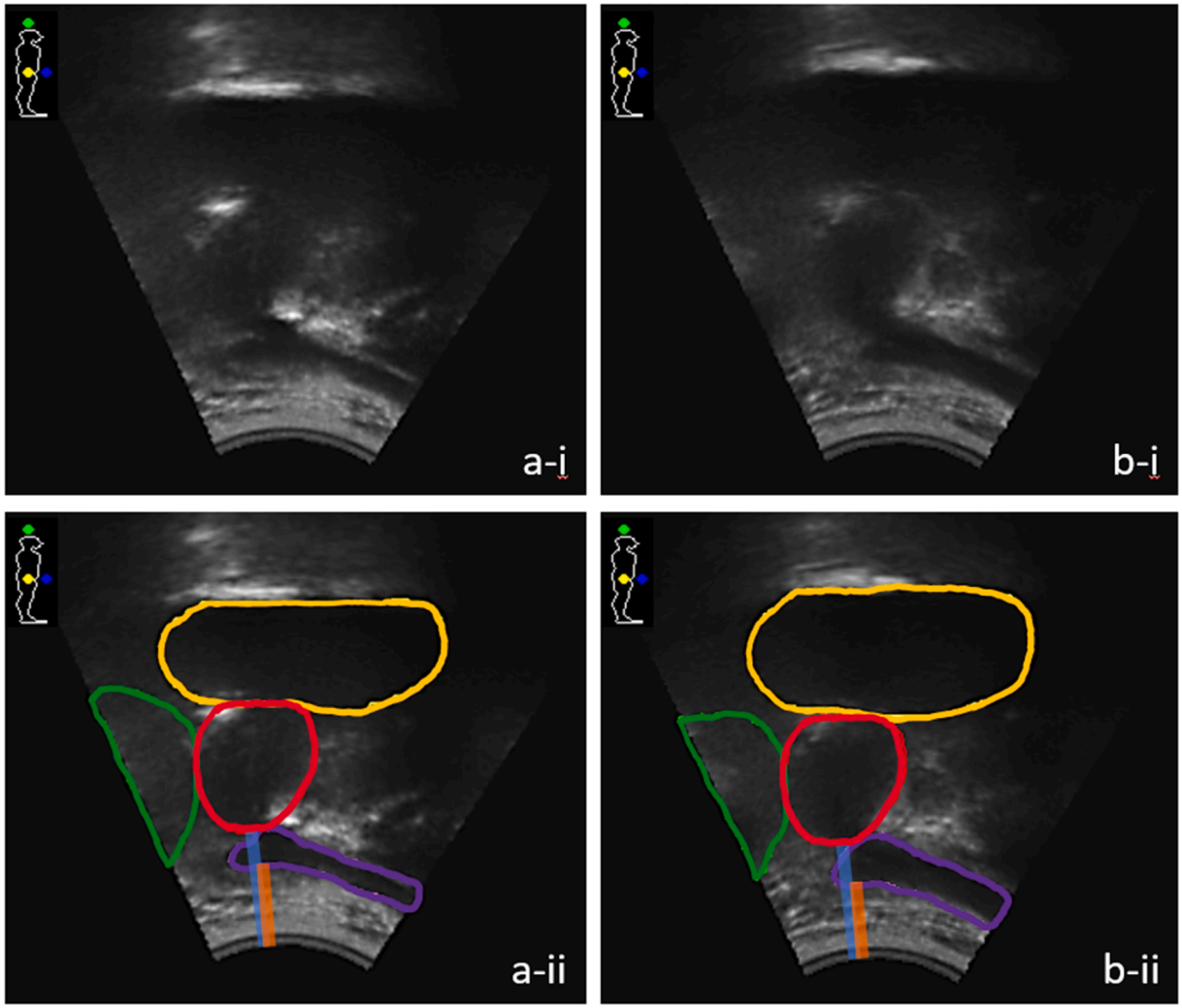

Fig. 3. Visual representation of tissue compression and corpus to prostate ratio (CPR), where the blue line represents the probe to prostate apex (PPA), and the orange line represents the probe to inferior corpus spongiosum (PICS). (a-i) shows greater compression of the US with (a-ii) highlighting the anatomy of prostate in red; corpus spongiosum in purple; bladder in yellow; and rectum in green. (b-i) shows compression released by 1.4 cm on the baseplate scale, with corresponding (b-ii) highlighting the relevant anatomy, as for (a-ii). The CPR in (a-ii) = 0.72 (2.1 cm/2.9 cm) and the CPR in b-ii = 0.63 (1.9/3.0 cm). These images were taken approximately 2 min apart, with no other changes apart from probe longitudinal position. (For interpretation of the references to colour in this figure legend, the reader is referred to the web version of this article.)

inferior edge of the corpus spongiosum identified 1 cm anterior to the middle of the probe surface. This was validated on the corresponding US dataset where the inferior edge of the corpus spongiosum can be clearly seen (Fig. 3). The prostate apex was located according to consensus guidelines for CT and MRI organ delineation [14].

Geometric coordinates of the probe surface, inferior corpus spongiosum and prostate apex were recorded in three dimensions (x,y,z). The Euclidean distance from the probe surface to the prostate apex was calculated (Eq. (2)). 'Px, Py, Pz' represents the probe position on the sagittal, transverse, and coronal planes, respectively. 'Ax, Ay, Az' represents the prostate apex position on the sagittal, transverse, and coronal planes, respectively. The same method was used to calculate the PICS distance (Eq. (3)). 'Ix, Iy, Iz' indicates the position of the inferior corpus spongiosum on the sagittal, transverse, and coronal planes respectively. All units were recorded in centimetres.

$$Probe\ to\ prostate\ apex\ distance = \sqrt{(Px-Ax)^2+(Py-Ay)^2+(Pz-Az)^2} \quad (2)$$

$$Probe\ to\ inf.\ corpus\ spongiosum = \sqrt{(Px-Ix)^2+(Py-Iy)^2+(Pz-Iz)^2} \quad (3)$$

Image rating

Each ultrasound image was categorised into ratings of 1, 2 or 3 according to an image quality assessment criteria (Table 1) defined by Camps et al (2020) [15]. One investigator (KDS) rated all images, with another investigator (AB) independently rating a subset (n = 15) as quality assurance.

Statistical methods

A statistical power analysis calculated a sample size of 93 patients, allowing for an 80% chance of identifying a statistically significant relationship between measurements and perineal dose. This was calculated based on pilot data of 20 patients. Statistical analysis was performed using R and the base R function - lm (R package version 3.6.2). Categorical variables (treatment technique and image rating score) were reported as percentages; continuous variables (age, BMI, Max perineum dose, PICS and CPR) were reported as mean ± SD (standard deviation) if normally distributed or as median (IQR interquartile range). To assess the statistical significance of predictors of perineal dose, multiple linear regression analysis was used. Stepwise regression, in forwards, backwards and both directions (R function StepAIC), was used to identify potential predictors in the model [16]. Decisions to include/exclude model predictors at each step were made by comparing the Akaike Information Criterion (AIC) values between models with and without the relevant predictor. The AIC is a measure of goodness of fit that penalises the number of parameters in the model [17]. A standardised residual and quantile–quantile (Q-Q) plot was created of the fitted model. Visual inspection of the residuals demonstrated that these were centred on zero with evidence of a constant variance (homoscedasticity). Variance Inflation Factor (VIF) was used to assess collinearity in multiple linear regression analysis. One-way ANOVA analysed the relationship between image-quality and PPA, PICS, CPR and BMI respectively. Findings were considered statistically significant at $P < 0.05$.

Table 1
Image quality assessment criteria for transperineal ultrasound images of the male pelvic region. The table was adapted from Camps et al (2020) [15].

Ultrasound Rating	Criteria
1	Prostate cannot be identified
2	Only the prostate or the prostate and either a part of the bladder or rectum could be identified
3	Prostate could be identified, as well as part of the bladder and the rectum

Results

115 prostate patient datasets met inclusion criteria and were analysed. The median age at treatment was 74.0 years (IQR 10). BMI values were available for 80 individuals (with 35 missing height and/or weight data). The median BMI at treatment was 29.57 m/kg^2 (IQR 8.36). The maximum dose to perineum ranged from 1.81 to 45.56 Gy, with a median of 5.87 Gy. Most participants (n = 95) recorded a maximum dose <10 Gy. 14 recorded a maximum dose between 10 and 20 Gy. However, two participants recorded a dose greater than 40 Gy. Most patients underwent IMRT or VMAT. Demographic and quality information is summarised in Table 2.

There was a linear correlation between CPR and PICS ($r = 0.65$, $p < 0.01$). All clinically relevant predictors were included in the initial model: BMI, treatment type, age, image rating, and anatomical compression (PICS and CPR). A detailed analysis of the stepwise regression dictated by the AIC value resulted in a model with two significant predictors of maximum perineal dose: PICS and CPR. Forwards and backwards stepwise regression confirmed this result – each of which selected the same model. To check there was no interaction between the distance terms PICS and CPR, an additional predictor (PICS × CPR) was added to the model; however, this did not improve on the final fitted model.

The adjusted R squared value in the model was 0.19 ($p < 0.001$), indicating the proportion of variance of maximum perineal dose that the model predictors can explain. The relative effect of each model predictor is represented graphically in Fig. 4, which displays the standardised regression coefficient of each model predictor. This graph demonstrates that a CPR approaching 1 and a reduction in PICS predicts increased perineal dose. The 95% confidence intervals for each regression coefficient do not include zero, suggesting that the variable effects are all significantly different from zero.

When other predictors were held fixed, dose was estimated to increase 8.82 Gy (95% CI 5.03–12.61, $p < 0.001$) on average, with a decrease of 1 cm of the PICS. Further, a 10% increase in the CPR resulted in an increased dose of 3.57 Gy (95% CI 2.00–5.10, $p < 0.001$). BMI, age, imaging type and image quality were not significant predictors of perineal dose.

There was 100% agreement in the subset of TPUS image quality rated independently by the two investigators. While there was a slight trend for increased image quality with decreased BMI, decreased PPA,

Table 2
Patient characteristics.

Specification		Median (IQR)	Number (% of total population)
Age (years)		74 (28)	
BMI (m/kg^2)		29.6 (8.35)	
Radiation treatment technique			
	IMRT		57 (49.6%)
	VMAT		50 (43.5%)
	3DCRT		8 (7%)
Max perineum dose (Gy)		5.87 (3.17)	
PICS distance (cm)		1.67 (0.63)	
CPR		0.51 (Range 1.29–0.88)	
US Image Rating Score	1		28 (24.3%)
	2		12 (10.4%)
	3		62 (53.9%)
	NR		13 (11.3%)

IQR = Interquartile range, BMI = Body Mass Index, PICS = Probe to inferior corpus spongiosum distance, CPR = Corpus to prostate ratio, US = Ultrasound; NR = Not recorded.

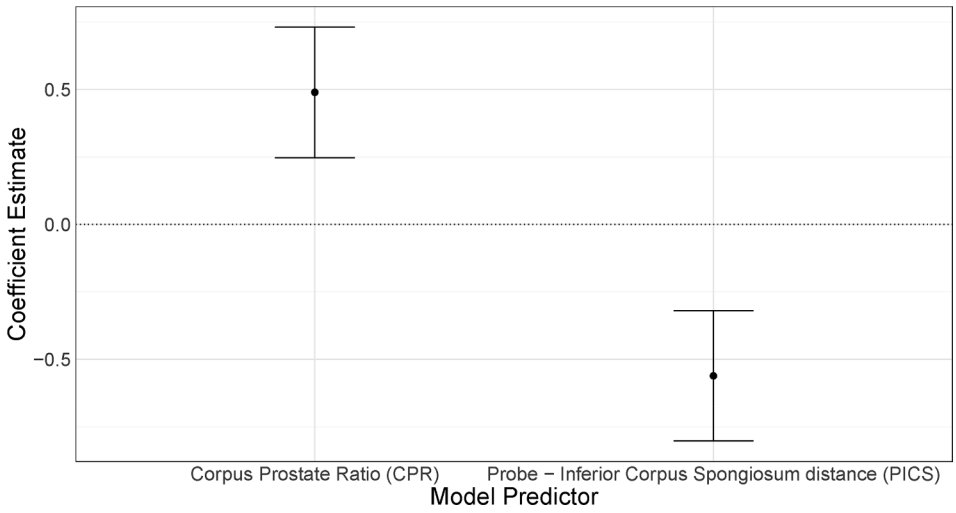

Fig. 4. Graphical comparison of standardised regression coefficients of model predictors, Corpus to Prostate Ratio (CPR) and Probe to Inferior Corpus Spongiosum distance (PICS).

PICS and CPR, these differences were not significant ($p < 0.05$ – see Supplementary Fig. 2a–d).

Discussion

Multiple linear regression analysis demonstrated a statistically significant association between the effects of increased anatomical compression (reduced PICS and increased CPR) and maximum perineal skin dose. To the authors' knowledge, this was the first study to investigate and quantify the impact of the Clarity TPUS anatomical compression on perineum skin dose.

In a similar study, Mantel et al. (2016) investigated the dosimetric impact of the Clarity TPUS probe on penile bulb dose [12]. When the probe was placed on the perineum, the study reported median penile bulb shifts of 1 mm posterior, 6 mm superior, with no relevant change to the prostate. The investigation concluded that the penile bulb was shifted into a higher dose region due to increased tissue compression from the ultrasound probe and received a greater dose [12]. The dose was more significant than the recommended penile bulb dose tolerance [18]. Consequently, a dose objective was implemented into the clinical protocol. Our study has focused specifically on the perineum skin and in keeping with the results of Mantel et al. (2016), [12] we also found that the compression from the TPUS probe increased dose to the perineum skin.

To attain good image quality and prostate localisation, a degree of tissue compression is required. However, increased anatomical compression was also associated with increased maximum perineal dose. Therefore, to achieve the optimal balance between adequate image quality and minimising excess perineal dose, current departmental guidelines recommend force is backed off at simulation as much as possible without compromising US quality. In this study, ultrasound image quality did vary between the three ratings, with approximately 25% of cases categorised into an image rating of 1, the poorest quality score. Image quality however, was not found to have an association with perineal dose, indicating that acceptable image quality can be achieved without increasing perineal dose.

There were no significant differences between image quality rating and measures of compression in our sample. Ultrasound imaging quality therefore is not solely dependent on probe pressure, as illustrated in Fig. 3 where different compressions both produced a good quality image. This provides some confidence that a reduction in probe pressure would not significantly adversely impact image quality. Image quality was judged on the ability to image the prostate and surrounding important landmarks, and is likely determined by a range of factors. Other techniques such as the application of more gel, repositioning the probe to a more suitable window or changing the probe angle or height may all be alternative ways to improve quality in an individual.

The prostate apex is challenging to locate on US and CT and prone to inter-user variability [19,20]. Consequently, the CPR ratio, which requires visualisation of the prostate apex, may also be deemed clinically impractical. The PICS distance was much easier to identify on US and CT, and from our observations, appeared less reliant on experience levels. In fact, from the modelling in this study, the PICS distance had a more significant influence on the perineal dose, making it a more useful indicator of excessive compression for radiation therapists to utilise clinically. Furthermore, our current department guidelines require the distance from the probe to the prostate apex to be 2 cm or greater. The findings from this investigation into perineal dose and tissue compression support this protocol, with a suggested update of incorporation of PICS of 1.2 cm or greater.

Skin toxicities such as moist desquamation are likely to be prominent at a skin dose greater than 40 Gy [13]. Therefore, tissue compression should be considered to minimise perineal dose. The majority of patients in this cohort (82.6%) recorded a maximum dose <10 Gy, with 12% recording a maximum dose of 10–20 Gy. However, two patients (1.7%) recorded greater than 40 Gy with the maximum dose at 45.56 Gy. No additional clinical indications (such as prostate volume) were found to explain these higher doses, except for the compression. Clinical notes for these patients were reviewed; fortunately, no skin toxicities during or post treatment were reported.

Furthermore, there was no statistically significant association between maximum perineum dose and BMI. BMI has poor specificity, and sensitivity and can be clinically misleading [21]. The measure does not consider tissue composition, and a high BMI does not necessarily indicate high adipose tissue deposition at the perineum.

The study was limited in assessing the statistical significance between the 3DCRT treatment technique and perineum doses. While there were 57 and 50 patients who had undergone IMRT and VMAT, respectively, only eight patients underwent 3DCRT. However, this has minimal clinical implications as 3DCRT is becoming increasingly obsolete, and most prostate patients today would undergo treatment with VMAT. While the inherent challenges with reproducibility of US is recognised, this is minimised with the daily positioning guide as part of the TPUS system. Nevertheless, differences in probe set-up including compression may have slightly varied the actual delivered dose, a limitation of this retrospective dosimetric assessment.

A potential consideration for future development of Elekta's Clarity Autoscan system would be the addition of a probe pressure indicator

that would alert the RT if tissue compression exceeded a pre-defined threshold. Though clinical staff can assess anatomical compression with measures such as the PICS distance or CPR, Pang et al (2017) concluded inter-observer variation with the Clarity system whilst minimal, appeared to be influenced by training and/or level of experience [22]. It is also expected that the avoidance of excessive compression will aide in continued patient comfort and tolerability [7,8].

Future directions

A potential prospective study could be conducted where the probe pressure is set to a feasible maximum (from both an individual anatomical and tolerability view) and then decreased in increments to assess the point at which image quality is sacrificed. This type of study would also be able to report visual indications that could be used clinically to identify excessive probe pressure. Ultrasound technology is also advancing rapidly and future improvements in image quality may allow radiation therapists to achieve better prostate visualisation in larger patients without applying significant probe pressure [23]. Furthermore, additional robotic and artificial intelligence may provide further benefits [24]. More broadly, this study highlights the need for such investigations when setups in radiation therapy are altered through technology or other means.

Conclusion

The main advantage of using real-time transperineal non-ionising ultrasound systems to monitor intrafraction prostate motion is improved treatment accuracy; however, radiation therapists utilising this technology should also consider the impact of tissue compression caused by probe positioning on perineum dose. Increasing compression has the potential to increase radiation-induced effects on non-target tissue. This study demonstrated that anatomical compression using PICS and CPR reference values is a statistically significant predictor of maximum perineal dose. Departments that utilise Clarity are encouraged to incorporate probe pressure considerations into clinical guidelines and protocols, with a recommended PICS of 1.2 cm or greater, with CPR reduced as much as possible without losing anatomical US definition. Additionally, departments utilising Clarity should consider contouring the perineum as standard practice and include the perineum within the radiation prescription as a standard dose reporting structure for prostate cancer patients.

Data sharing statement

Research data are stored in an institutional repository and will be shared upon request to the corresponding author.

Declaration of Competing Interest

The authors declare that they have no known competing financial interests or personal relationships that could have appeared to influence the work reported in this paper.

Acknowledgements

Thank you to the Townsville Cancer Centre for their support in conducting this study. A special thank you to Dr Chris Rumley (radiation oncologist) and Christine Albantow (radiation therapist) for their assistance and guidance during the data collection process.

Appendix A. Supplementary material

Supplementary material to this article can be found online at https://doi.org/10.1016/j.tipsro.2022.08.003.

References

[1] Roch M, Zapatero A, Castro P, Büchser D, Pérez L, Hernández D, et al. Impact of rectum and bladder anatomy in intrafractional prostate motion during hypofractionated radiation therapy. Clin Transl Oncol 2019;21(5):607–14.
[2] Grimwood A, McNair HA, O'Shea TP, Gilroy S, Thomas K, Bamber JC, et al. In Vivo Validation of Elekta's Clarity Autoscan for Ultrasound-based Intrafraction Motion Estimation of the Prostate During Radiation Therapy. Int J Radiat Oncol Biol Phys 2018. https://doi.org/10.1016/j.ijrobp.2018.04.008.
[3] Camps S, Edwards C. Ultrasound for measuring interfraction organ motion. In: Harris E, Fontanarosa D, Camps S, Verhaegen F, editors. Modern Applications of 3D/4D Ultrasound Imaging in Radiotherapy, IOP Publishing; 2021, p. 6–1 to 6–14. https://doi.org/10.1088/978-0-7503-2552-3.
[4] Azcona JD, Xing L, Chen X, Bush K, Li R. Assessing the dosimetric impact of real-time prostate motion during volumetric modulated arc therapy. Int J Radiat Oncol Biol Phys 2014;88:1167–74. https://doi.org/10.1016/j.ijrobp.2013.12.015.
[5] Barnett GC, West CML, Dunning AM, Elliott RM, Coles CE, Pharoah PDP, et al. Normal tissue reactions to radiotherapy: towards tailoring treatment dose by genotype. Nat Rev Cancer 2009;9(2):134–42.
[6] Camps SM, Fontanarosa D, de With PHN, Verhaegen F, Vanneste BGL. The Use of Ultrasound Imaging in the External Beam Radiotherapy Workflow of Prostate Cancer Patients. Biomed Res Int 2018;2018:1–16.
[7] Pang EPP, Knight K, Baird M, Loh JMQ, Boo AHS, Tuan JKL. A comparison of interfraction setup error, patient comfort, and therapist acceptance for 2 different prostate radiation therapy immobilization devices. Adv Radiat Oncol 2016;2:1–7. https://doi.org/10.1016/j.adro.2017.02.001.
[8] Brown A, Pain T, Preston R. Patient perceptions and preferences about prostate fiducial markers and ultrasound motion monitoring procedures in radiation therapy treatment. J Med Radiat Sci 2021;68:37–43. https://doi.org/10.1002/JMRS.438.
[9] Johnson MH, Chang A, Brandes SB. The value of digital rectal examination in assessing for pelvic fracture associated urethral injury: What defines a high-riding or nonpalpable prostate? J Trauma Acute Care Surg 2013;75:913–5. https://doi.org/10.1097/TA.0b013e3182a68668.
[10] Li M, Hegemann N-S, Manapov F, Kolberg A, Thum PD, Ganswindt U, et al. Prefraction displacement and intrafraction drift of the prostate due to perineal ultrasound probe pressurePräfraktionelle Verschiebung und intrafraktionelle Drift der Prostata durch Druck perinealer Ultraschallköpfe. Strahlenther Onkol 2017;193(6):459–65.
[11] Pang EPP, Knight K, Leung R-K, Wang MLC, Chan JWS, Low GK, et al. Technical considerations for positioning and placement of a transperineal ultrasound probe during prostate radiotherapy. J Med Radiat Sci 2021;68(2):196–202.
[12] Mantel F, Richter A, Groh C, Lawrenz I, Weick S, Polat B, et al. Changes in penile bulb dose when using the Clarity transperineal ultrasound probe: A planning study. Pract Radiat Oncol 2016;6(6):e337–44.
[13] Wei J, Meng L, Hou X, Qu C, Wang B, Xin Y, et al. Radiation-induced skin reactions: Mechanism and treatment. Cancer Manage Res 2019;11:167–77. https://doi.org/10.2147/CMAR.S188655.
[14] Salembier C, Villeirs G, De Bari B, Hoskin P, Pieters BR, Van Vulpen M, et al. ESTRO ACROP consensus guideline on CT- and MRI-based target volume delineation for primary radiation therapy of localized prostate cancer. Radiother Oncol 2018;127(1):49–61.
[15] Camps SM, Houben T, Carneiro G, Edwards C, Antico M, Dunnhofer M, et al. Automatic Quality Assessment of Transperineal Ultrasound Images of the Male Pelvic Region, Using Deep Learning. Ultrasound Med Biol 2020;46(2):445–54.
[16] Hocking RR. A Biometrics Invited Paper. The Analysis and Selection of Variables in Linear Regression. Biometrics 1976;32(1):1.
[17] Harrell FE. Regression Modeling Strategies. Cham: Springer International Publishing; 2015. https://doi.org/10.1007/978-3-319-19425-7.
[18] Roach M, Nam J, Gagliardi G, El Naqa I, Deasy JO, Marks LB. Radiation Dose-Volume Effects and the Penile Bulb. Int J Radiat Oncol Biol Phys 2010;76(3):S130–4.
[19] Li X-M, Gao X-S, Guo X-M, Li Y-G, Wang X-Y. Using CT imaging to delineate the prostatic apex for radiation treatment planning. Chinese J Cancer 2010;29:914–22. https://doi.org/10.5732/cjc.010.10193.
[20] Shanker MD, Kim ANH, Brown A, Tan AHM. Anatomical and dosimetric assessment of the prostate apex: A pilot comparison of image-guided transperineal ultrasound to conventional computed tomography simulation. J Med Imag Radiat Oncol 2020;64:839–44. https://doi.org/10.1111/1754-9485.13045.
[21] Rothman KJ. BMI-related errors in the measurement of obesity. Int J Obesity 2008;32:S56–9. https://doi.org/10.1038/ijo.2008.87.
[22] Pang EPP, Knight K, Baird M, Tuan JKL. Inter- and intra-observer variation of patient setup shifts derived using the 4D TPUS Clarity system for prostate radiotherapy. Biomed Phys Eng Express 2017;3(2):025014.
[23] Sriharsha GMD, John EP, Jingzhi LMD, Zhaojun LMD, Flemming FP, Andrej LMD, et al. Advances in Modern Clinical Ultrasound. Adv Ultrasound Diagn Therapy 2018;2(2):51.
[24] Edwards C, Chamunyonga C, Searle B, Reddan T. The application of artificial intelligence in the sonography profession: Professional and educational considerations. Ultrasound 2022;15:1742271X2110724. https://doi.org/10.1177/1742271X211072473.